Reduction of monsoon rainfall in response to past and future land use and land cover changes

Benjamin Quesada, Narayanappa Devaraju, Nathalie Noblet-ducoudré, Almut Arneth

AGU PUBLICATIONS

Geophysical Research Letters

RESEARCH LETTER
10.1002/2016GL070663

Key Points:
- Effects of land use and land cover changes (LULCC) on past and future monsoon rainfall are assessed in eight monsoon regions
- Biophysical effects of LULCC contribute to weaken by ~30% monsoon rainfall projections
- Importance of considering LULCC in past and future hydrological cycle assessment

Supporting Information:
- Figures S1–S9 and Tables S1–S3

Correspondence to:
B. Quesada,
benjamin.quesada@kit.edu

Citation:
Quesada, B., N. Devaraju, N. de Noblet-Ducoudré, and A. Arneth (2017), Reduction of monsoon rainfall in response to past and future land use and land cover changes, *Geophys. Res. Lett.*, *44*, 1041–1050, doi:10.1002/2016GL070663.

Received 31 JUL 2016
Accepted 30 NOV 2016
Accepted article online 5 DEC 2016
Published online 30 JAN 2017

Reduction of monsoon rainfall in response to past and future land use and land cover changes

Benjamin Quesada[1], Narayanappa Devaraju[2], Nathalie de Noblet-Ducoudré[2], and Almut Arneth[1]

[1]Institute of Meteorology and Climate Research, Atmospheric Environmental Research, Karlsruhe Institute of Technology, Garmisch-Partenkirchen, Germany, [2]Laboratoire des Sciences du Climat et de l'Environnement LSCE/IPSL, Unité mixte CEA-CNRS-UVSQ, Université Paris-Saclay, Gif-sur-Yvette, France

Abstract Land use and land cover changes (LULCC) can have significant biophysical impacts on regional precipitation, including monsoon rainfall. Using global simulations with and without LULCC from five general circulation models, under the Representative Concentration Pathway 8.5 scenario, we find that future LULCC significantly reduce monsoon precipitation in at least four (out of eight) monsoon regions. While monsoon rainfalls are likely to intensify under future global warming, we estimate that biophysical effects of LULCC substantially weaken future projections of monsoons' rainfall by 9% (Indian region), 12% (East Asian), 32% (South African), and 41% (North African), with an average of ~30% for projections across the global monsoon region. A similar strong contribution is found for biophysical effects of past LULCC to monsoon rainfall changes since the preindustrial period. Rather than remote effects, local land-atmosphere interactions, implying a decrease in evapotranspiration, soil moisture, and clouds along with more anticyclonic conditions, could explain this reduction in monsoon rainfall.

1. Introduction

Land use and land cover changes (LULCC) alter surface energy, momentum, heat, water, and biogeochemical balances (e.g., CO_2 emissions). Several modeling experiments [*Gupta et al*., 2005; *Abiodun et al*., 2008; *Takata et al*., 2009; *Devaraju et al*., 2015; *Halder et al*., 2015] and observational studies [*Webb et al*., 2005; *Pielke et al*., 2007; *Lee et al*., 2009; *Kishtawal et al*., 2010; *Niyogi et al*., 2010] analyzed the links between LULCC and monsoon perturbations, especially in Asia [*Pielke et al*., 2011]. For instance, with remote sensing satellite observations, *Niyogi et al*. [2010] could partly attribute a significant decline in Indian summer monsoon rainfall in the past decades to an agricultural intensification in this region. *Takata et al*. [2009] argued that local LULCC during a preindustrial period (1700–1850) was the major anthropogenic disturbance that weakened the Asian summer monsoon. In response to idealized deforestation scenarios, monsoon rainfall decreased in Africa and the northern parts of India but increased in southern India [*Gupta et al*., 2005]. *Devaraju et al*. [2015] simulated a decline in Northern Hemisphere monsoon rainfall particularly in South Asia (−11% and−12% for annual and boreal summer precipitation, respectively) and an increase in Southern Hemisphere monsoon rainfall in response to a global-scale deforestation experiment. But when deforestation was restricted to tropical latitudes (20°S–20°N), they found only small effects on monsoon rainfall. In a regional analysis, *Halder et al*. [2015] found that observed LULCC over India during recent decades has contributed to a decline in Indian summer monsoon rainfall through changes in large-scale circulations and decrease in moisture convergence.

However, a common feature is shared by all these modeling studies: they are based on the use of only one global or regional climate model and/or they apply different idealized deforestation/afforestation scenarios (e.g., 100% or 50% of forests replaced by crops or grasslands, and vice versa). Thus, review studies have called for climate model intercomparisons to validate the LULCC impacts on monsoon rainfall since results are overall inconclusive [*Pielke et al*., 2011; *Mahmood et al*., 2014; *Lawrence and Vandecar*, 2015; *Xue and Dirmeyer*, 2015]. To our knowledge, only *Pitman et al*. [2009] and *Brovkin et al*. [2013] have investigated past and future LULCC impacts in a multimodel framework, and they did not find statistically significant changes in global mean precipitation. Therefore, interactions between LULCC and monsoon are often not robustly simulated, and a quantification of the hydrological cycle sensitivity to LULCC is still missing [*Pielke et al*., 2011; *Xue and Dirmeyer*, 2015].

Moreover, while scientists widely agree on robust local climate effects and remote biogeochemical effects through changes in atmospheric CO_2 concentration [see *Pielke et al*., 2011; *Mahmood et al*., 2014; *Lawrence*

and Vandecar, 2015, and references therein], remote biophysical effects (i.e., teleconnections through large-scale variations of the atmosphere's water and energy budget) are still debated [*Chase et al*., 2000; *Werth and Avissar*, 2002; *Avissar and Werth*, 2005; *Findell et al*., 2006, 2009; *Pitman et al*., 2009; *Snyder*, 2010; *Pielke et al*., 2011; *Mahmood et al*., 2014]. For instance, whether or not significant effects on rainfall also arise outside the deforested areas has not yet been consistently shown [*Pitman et al*., 2009; *Pielke et al*., 2011; *Brovkin et al*., 2013; *Mahmood et al*., 2014; *Lawrence and Vandecar*, 2015]. Thus, local and/or remote effects of LULCC could contribute to modulate monsoon rainfall.

For the first time here, using several global coupled simulations and realistic global LULCC scenarios, we quantify the likely impacts of past and future LULCC on rainfall in all the world's monsoon regions in which more than 70% of world's population reside (section 3.1). Finally, we investigate the underlying physical mechanisms (remote versus local land-atmosphere interactions) between LULCC and monsoon (section 3.2) which are still not consensual.

2. Methods

2.1. Monsoon Regions

Eight (8) regions are defined as regional monsoon precipitation domains. Those are regions where (i) the annual range of precipitation rates exceeds 2 mm/d (or 300 mm per season) and (ii) the local summer precipitation exceeds 55% of the total annual rainfall [see *Yim et al*., 2014, Figure 1]. Then the associated rectangular domains of regional monsoons with their names, initials, and geographical definition—terminology and domains are from *Yim et al*. [2014]—are the following: Indian IN (10°N–30°N, 70°E–105°E), Western North Pacific WNP (12.5°N–22.5°N, 110°E–150°E), East Asia EA (22.5°N–45°N, 110°E–135°E), North America NAM (7.5°N–22.5°N, 110°W–80°W), Northern Africa NAF (5°N–15°N, 30°W–30°E), South America SAM (5°S–25°S, 70°W–40°W), Southern Africa SAF (7.5°S–25°S, 25°E–70°E), and Australia AUS (5°S–20°S, 110°E–150°E) (see eight regions in supporting information, Figures S1 and S2). Similar domains have already been used in other studies [*Wang and Ding*, 2006, 2008; *Kitoh et al*., 2013]. Figure S2 shows the local projected annual range of precipitation rates, as defined in *Yim et al*. [2014], only when local summer precipitation exceeds 55% of the total annual rainfall. We confirm that climate models simulate correctly the above mentioned regions that encompass most monsoon rainfall. The "global monsoon region" [*Trenberth et al*., 2000; *Wang and Ding*, 2008] refers in our study to a virtual domain aggregating these eight monsoonal domains. The robustness of our results to other different monsoon domains is tested in section 3.2.

2.2. Intertropical Convergence Zone Shifts

Shifts in the Intertropical Convergence Zone (ITCZ) are diagnosed using the "precipitation centroid" metric [*Donohoe et al*., 2014; *Devaraju et al*., 2015] that allows to calculate the latitudinal location of the ITCZ precipitation maximum. The precipitation centroid is then defined as the median of the zonally averaged precipitation between 20°S and 20°N. This zonal mean precipitation is interpolated to 0.01° resolution which allows the precipitation centroid to vary at increments smaller than the grid spacing of the model simulations (~2° longitude × 2° latitude) [*Donohoe et al*., 2014; *McGee et al*., 2014; *Devaraju et al*., 2015; *Adam et al*., 2016]. ITCZ shifts are thus defined as meridional shifts (in °N) of the precipitation centroid location.

2.3. Models and Experiments

The Land Use and Climate, Identification of Robust Impacts (LUCID) is a major international intercomparison exercise that intends to diagnose the robust biophysical impacts of LULCC using as many climate models as possible forced with same LULCC (http://www.lucidproject.org.au/).

2.3.1. LUCID-CMIP5 (Effects of Future LULCC)

The LUCID-Coupled Model Intercomparison Project (CMIP5) simulations analyzed here are the same as those described in *Brovkin et al*. [2013] and *Boysen et al*. [2014]. Focusing on the impacts of future changes of LULCC, several modeling groups from the fifth Phase of the Coupled Model Intercomparison Project (CMIP5) performed LUCID-CMIP5 simulations without anthropogenic land use changes from 2006 to 2100. Here we use outputs from the five LUCID-CMIP5 and CMIP5 models (CanESM2, HadGEM2-ES, IPSL-CM5A-LR, MPI-ESM-LR, and MIROC-ESM) on the last 30 years period of each experiment (2071–2100). Representative Concentration Pathway 8.5 (RCP8.5) simulations are the CMIP5 runs with all forcings including the future

anthropogenic land use and land cover change forcing based on RCP8.5 scenario. L2A85 simulations are the same runs as RCP8.5 but without the anthropogenic land use and land cover change forcing (after year 2005), with atmospheric CO_2 concentration prescribed from the RCP8.5 scenario. In other means, the difference between RCP8.5 and L2A85 simulations (i.e., RCP8.5-L2A85) corresponds to the pure biophysical effects of future anthropogenic land use and land cover changes. Note that the RCP8.5 scenario includes spatially explicit future LULCC characterized by an expansion of croplands and pastures driven by the food demands of an increasing population and corresponds to a radiative forcing of more than 8.5 $W m^{-2}$ in 2100 [*Hurtt et al*., 2011] (CO_2 concentration ~ 936 ppm in 2100). Future changes in tree cover between RCP8.5 and L2A85 simulations are about 4×10^6 km^2 by 2100 (i.e., approximately one tenth of the total idealized deforestation scenarios [*Ward et al*., 2014]). Harmonization and implementation of future LULCC scenario into these five CMIP5 models are fully detailed in *Hurtt et al*. [2011] and *Brovkin et al*. [2013] papers (see their sections 2a and 2b).

For the analysis of the changes in surface energy components and land-atmosphere variables (CMIP5 standard abbreviation in parenthesis), we used the sensible and latent heat fluxes (hfss and hfls), incoming shortwave and longwave radiation at the surface (rsds and rlds), total cloud fraction (clt), moisture in the upper portion of the soil column (mrsos), geopotential height, and vertical pressure velocity at 500 hPa (zg and wap) from RCP8.5 and L2A85 simulations averaged over the 2071–2100 period (Figure 3). Only wap variable for HADGEM2-ES model was not available.

2.3.2. LUCID (Effects of Past LULCC)

To investigate the impacts of LULCC since the preindustrial period, we also analyze LUCID simulations. Those have been used in previous studies: among others *Pitman et al*. [2009], *de Noblet-Ducoudré et al*. [2012], and *Boisier et al*. [2012]. In the standard present-day simulations (experiment PD) all greenhouse gases, land cover, and sea surface temperatures (SSTs) are prescribed at their present-day values. The land cover is prescribed using a map reflecting 1992 conditions (with vegetation distribution of *Ramankutty and Foley* [1999] for crops and *Goldewijk* [2001] for pastures) as being representative for the simulation period 1972–2002. The simulations were run by seven general circulation models (GCMs): ARPEGE, CCAM, CCSM, EC-EARTH, ECHAM5, IPSL, and SPEEDY. Similar simulations as PD but with a land cover map reflecting 1870 conditions were performed (experiment PDv). The difference between PD and PDv corresponds to the biophysical impacts of past LULCC. We also used the preindustrial simulations carried out in LUCID project (experiment PI). In PI, all greenhouse gases, land cover, and sea surface temperatures (SSTs) are prescribed at their preindustrial values (~1870). The land cover is prescribed using a map reflecting 1870, and the period 1870–1900 is simulated (same references than above for the vegetation distributions). The difference between PD and PI corresponds to the changes due to all forcings. Harmonization and implementation of past LULCC scenario into these seven climate models are fully detailed in methodology sections of *Pitman et al*. [2009] and *de Noblet-Ducoudré et al*. [2012].

For each set of simulations (PI, PD, and PDv), five independent realizations were run by each climate model and the average among these ensembles corresponds to the response of each model. For these sets, only land values were available, preventing ITCZ location calculation for this data set.

To calculate the contribution of future LULCC to precipitation projections, we also use historical precipitation data (HIST) from the five LUCID-CMIP5 models for 1976–2005 period. Projected changes in precipitation found by a previous study analyzing 21 CMIP5 climate monsoon projections [*Kitoh et al*., 2013] are consistent with the five LUCID-CMIP5 model (ENS-FUT) projections (Pearson correlation coefficient $r = 0.9$) with only a slight underestimation among the common monsoon regions (bias = 0.14 ± 0.25 mm/d, see Table S1).

Note that irrigation potential, landscape management practices, dust emissions from land use, and urbanization are not taken into account here in the implementation of the past and future LULCC scenarios.

Changes in "monsoon rainfall" depict here seasonal changes in precipitation: in December-January-February (DJF) for Southern Hemisphere regions (SAM, SAF, and AUS) and June-July-August (JJA) for Northern Hemisphere regions (IN, WNP, EA, NAM, and NAF). ENS-FUT refers to the ensemble mean from the five LUCID-CMIP5 models and ENS-PAST refers to the ensemble mean from the seven LUCID models.

2.4. Robustness and Statistical Significance

Two measures are implemented to analyze the likely effects of LULCC and discuss statistical significance: (i) model agreement on direction of change and (ii) statistical significance of simulated changes. A first

significance test is passed when at least 80% (70%) of the LUCID-CMIP5 (LUCID) model simulations and the multimodel mean ensemble ENS-FUT (ENS-PAST) display significant changes at 90th confidence level. For spatial precipitation averages, an additional significance test is performed to check whether at least 80% (70%) of the LUCID-CMIP5 (LUCID) model simulations show significant changes at 66th, 75th, or 80th confidence level. For these significance tests, we use the Mann-Whitney-Wilcoxon test [*Hollander and Wolfe*, 1999] with two sets of 30 year future simulations (e.g., RCP8.5 and L2A85 simulations, on 2071–2100 period). This test is widely used in many regional climate studies [*Haensler et al*., 2013; *Jacob et al*., 2014; *Thober and Samaniego*, 2014; *Pfeifer et al*., 2015]. Moreover, the Mann-Whitney-Wilcoxon test does not presume the distribution shapes of the samples which make this test particularly suited for precipitation data (right-skewed distributions) compared to, for example, a Student *t* test.

3. Results

Here we systematically investigate the effects of future LULCC on monsoon rainfall over eight monsoonal regions under the RCP8.5 scenario, using global simulations of five GCMs from the intercomparison projects CMIP5 and LUCID-CMIP5 (see section 2). The five GCMs mostly agree on the tropical deforestation signal, while model spread at higher latitudes is larger due to the different implementation of a common LULCC scenario among the models (dynamic versus nondynamic vegetation models) [*Brovkin et al*., 2013; *Boysen et al*., 2014]. In particular, in the eight monsoonal regions, models simulate local deforestation, except in eastern Asia (see Figure S1). The largest areas of deforestation are estimated to occur in southern America, southern Africa, and northern Africa with ensemble mean changes in tree cover being up to −25% by 2100.

3.1. LULCC-Induced Monsoon Rainfall Weakening

When considering only the effects of LULCC at the end of the 21st century, we find that biophysical effects of future LULCC significantly reduce monsoon rainfall, as seen in the decline by about 1–2% in precipitation in five monsoon regions (Figure 1; grey bars for Indian, South American, East Asian, Northern, and South African regions with green tick marks and circles for significance). Ensemble mean future changes (ENS-FUT) in seasonal precipitation vary from −0.14 mm/d (−2.6% in North America) to +0.06 mm/d (+0.7% in Western North Pacific). Spatially, most grid points across monsoonal regions show reduced precipitation patterns, except for Australia and Western North Pacific (Figure 2). In the Indian region, patterns are heterogeneous with declines in monsoon rainfall up to −0.5 mm/d are found in the eastern part of India and Bangladesh, as well as in the Arabian Sea and Bay of Bengal but some significant increases elsewhere. The eastern parts of South America, South Africa, and East Asia (China) are also significantly depleted in precipitation during monsoon seasons (Figure 2, black crosses for significance). Overall, in the global monsoon region (average among all eight monsoon regions), land-only changes are stronger than land + ocean changes, with a 1.9% reduction in monsoon rainfall but reaching up to −3% (South Africa, Western North Pacific, and North Africa, see grey bars in Figure S3). Although these precipitation changes appear small, they are significant and meaningful because they can have profound impacts on monsoon regions' economy [*Gadgil and Gadgil*, 2006], agricultural yields [*Auffhammer et al*., 2012], and water resources [*Tiwari and Joshi*, 2013]. Note also that a robust 1–2% increase in global mean precipitation is associated with a substantial global surface warming of ~1°K in response to greenhouse gas forcing [*Held and Soden*, 2006; *Trenberth*, 2011].

Furthermore, when LULCC effects on the monsoon change between present day and future are considered versus the effects of all forcings (RCP8.5-L2A85 versus RCP8.5-HIST, see section 2), the relative monsoon response becomes much more prominent (blue bars in Figure 1). Under the RCP8.5 scenario, monsoonal rainfall is projected to significantly increase in most regions (Table S1) as reported by previous studies [*Intergovernmental Panel on Climate Change* (*IPCC*), 2013; *Kitoh et al*., 2013]. Therefore, biophysical effects of LULCC contribute to significantly weaken the projections of monsoon rainfall in at least four regions: by 9% in the Indian region, 12% in the East Asian region, 32% in the South African region, and 41% in the North African region (Figure 1, blue bars). In South America, a strong negative contribution of biophysical effects of LULCC is found (~ −160%, Figure 1 blue bar) but not significant because South America is the only monsoon region where ENS-FUT monsoon rainfall projections are not significant (see Table S1, $p > 0.1$). Likewise, when considering only land grid points in monsoonal regions, biophysical effects of LULCC significantly lessen future projections of monsoon rainfall by 39% in South Africa, 24% in Western North Pacific, and 31% in

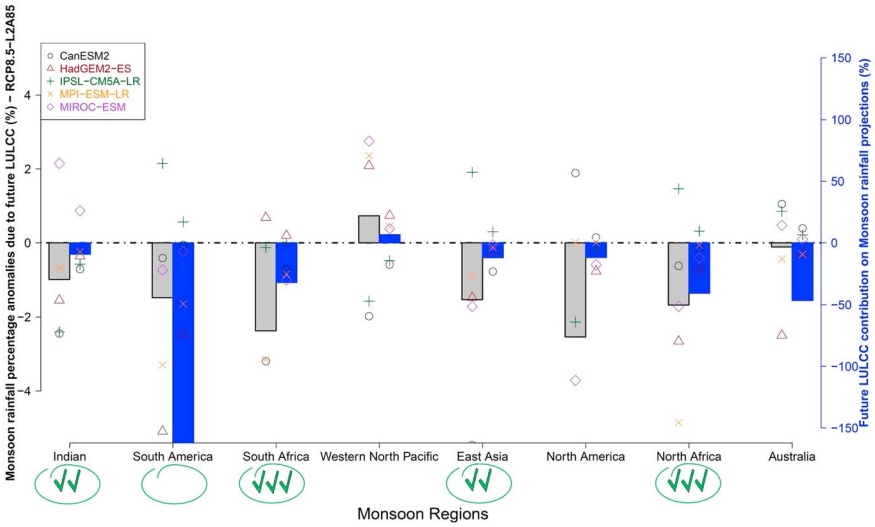

Figure 1. ENS-FUT changes in monsoon rainfall and their relative contribution to future projections (RCP8.5-HIST) in the eight monsoonal regions. Results are shown in DJF for Southern Hemisphere regions and in JJA for Northern Hemisphere regions averaged over 2071–2100 period. On the left axis, grey bars indicate monsoon rainfall anomaly percentage $\left(\frac{\text{RCP8.5}-\text{L2A85}}{\text{RCP8.5}}\right)$ due to future LULCC. On the right axis, blue bars indicate the contribution of future LULCC (RCP8.5-L2A85) relative to future projections with all forcings (RCP8.5-HIST). Both units are percent. Symbols are shown for individual results of each LUCID-CMIP5 model. Note that simulated precipitations are first arithmetically averaged among the five LUCID-CMIP5 models before the calculation of the rainfall anomaly percentage and the relative contribution. Statistical significance is given by green tick marks and circles. One, two, and three green tick marks are displayed for the regions where at least 80% of LUCID-CMIP5 models have regional changes significant at 66th, 75th, and 80th confidence level, respectively (see section 2). Green circles are added when ENS-FUT regional values are also significant at 90th confidence level.

North Africa, on average (red bars in Figure S3). On average, while global monsoon rainfall is simulated to increase at the end of the 21st century (see Table S1), biophysical effects contribute to decrease by ~30% these projected changes.

Interestingly, in our analysis, the two LUCID-CMIP5 models that are among the best CMIP5 models in simulating present-day monsoon precipitation [*Lee and Wang*, 2014] (CanESM2 and HadGEM2-ES) are also the models that project the highest decreases in global monsoon rainfall due to LULCC (respectively, −0.10 and −0.16 mm/d, i.e., −1.4% and −2.4%). Moreover, here, they give larger LULCC contributions to monsoon rainfall projections (−65% and −70% respectively) than the ensemble mean (−30%).

In addition, we find some evidence of shorter monsoon duration with significant changes in onset and retreat dates in some regions (see Table S2, using the fixed threshold method [*Wang and LinHo*, 2002]). In the Indian, Southern African, and Western North Pacific regions, most models simulate a decrease in the monsoon period duration (−4.2, −2.6, and −0.7 days on average, respectively).

We compare the changes in monsoon rainfall due to future LULCC with the ones due to past LULCC, using outputs from the seven global climate models of the LUCID project (see section 2). This comparison suggests that future LULCC have larger impacts on monsoon rainfall reduction than past LULCC (1992 minus 1870 vegetation maps, Figure S4). In most monsoon regions, we calculate that past LULCC reduce monsoon rainfall in at least six regions (grey bars in Figure S5), but simulated changes are significant only in the Indian (−0.04 mm/d, i.e., −0.5% on average) and South American (−0.05 mm/d, i.e., −0.4%) regions. Spatially, precipitation reductions due to past LULCC are significant in monsoon subregions of Northern India, South America, East Asia, and Northern Australia, up to −0.5 mm/d (Figure S6). In the Indian and South American regions, the relative contribution of past LULCC to past changes in precipitations is −47% and −33%, respectively (orange bars in Figure S5). Note that across the global monsoon region, the relative mean contribution of LULCC versus all forcings to past monsoon rainfall changes (PD-PDv versus PD-PI, see section 2) is ~−33%, which is about equal to the relative contribution of future LULCC (~−30%, as discussed earlier).

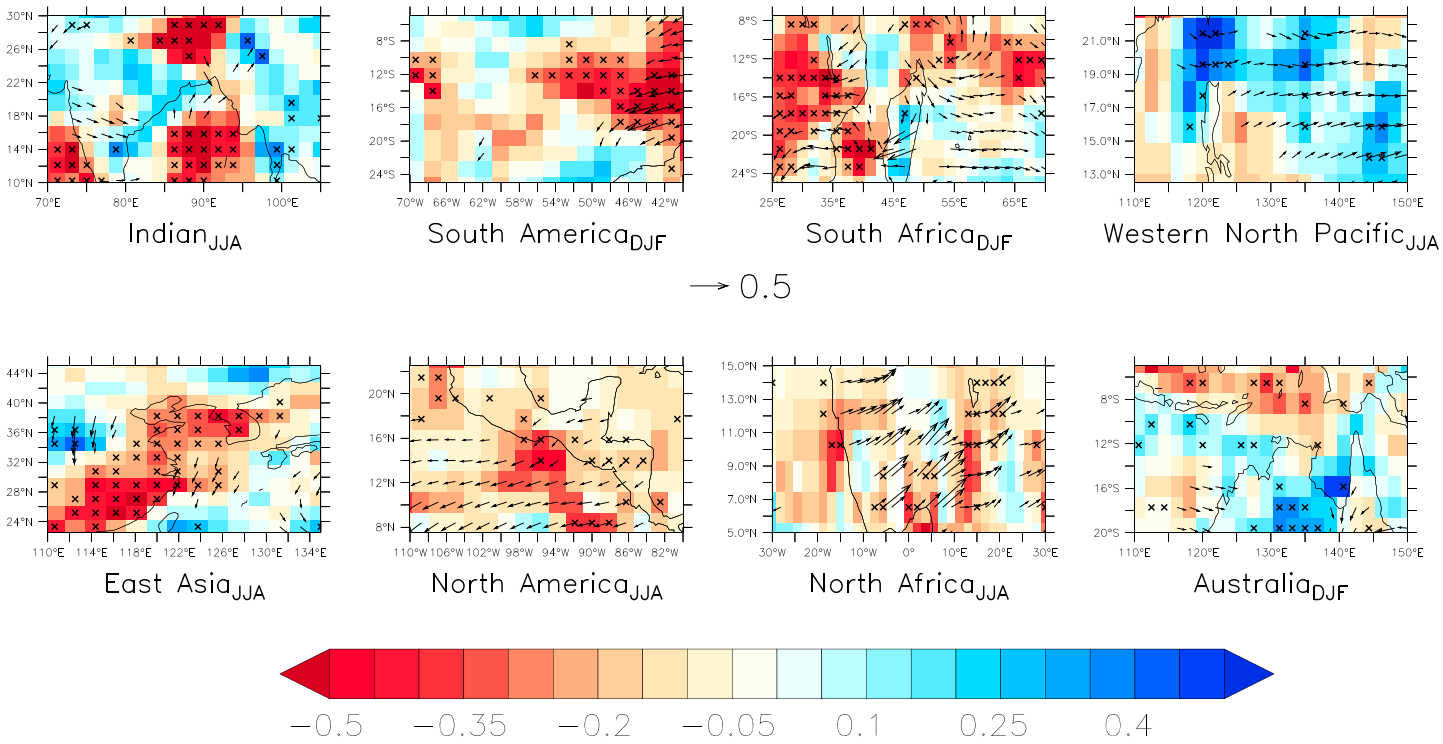

Figure 2. Spatial patterns of ENS-FUT changes in monsoon rainfall in the eight monsoonal regions. Black crosses are shown when at least 80% of LUCID-CMIP5 models simulate the same anomaly sign and ENS-FUT value is significant at 90th confidence level. Units for precipitation are mm/d. Arrow vectors correspond to changes in surface wind speed components (only wind speed changes greater than 0.1 m/s are displayed). Units for wind speed are m/s. Differences (RCP8.5-L2A85) are calculated for DJF in Southern Hemisphere regions and for JJA in Northern Hemisphere regions averaged over 2071–2100 period.

3.2. Remote Versus Local Land-Atmosphere Interactions

Numerous studies have suggested that remote biophysical effects of LULCC could affect regional precipitation through a shift in major features of the climate system that modulates rainfall amount [*Zheng and Eltahir*, 1997; *Medvigy et al.*, 2010; *Swann et al.*, 2012; *Devaraju et al.*, 2015; *Smith et al.*, 2016]. For example, LULCC can modulate the strength, timing, and location of the Hadley or Ferrel cell branches which further impact monsoon regimes [*Zhang et al.*, 1996; *Chase et al.*, 2000; *Feddema et al.*, 2005; *Snyder*, 2010; *Badger and Dirmeyer*, 2015]. Here we find little significant changes in the zonal mean meridional mass stream function due to future LULCC (Figure S7). In JJA, we find a small weakening in the rising branch of the Hadley cell but no significant changes in Hadley and Ferrel cells during DJF and at annual scale in response to future LULCC. This tends to indicate a nonsignificant and minor impact of changes in large-scale upper atmosphere circulations on global monsoon rainfall. Besides, all eight monsoon regions are located near the position of the ITCZ, and ITCZ shifts could therefore have strong impacts on the regional precipitation regime [*Medvigy et al.*, 2010; *Devaraju et al.*, 2015]. However, in our analysis, models simulate on average a slight southward ITCZ shift of 0.19° during JJA and almost no displacement during DJF and at annual scale (0.05° and 0.00° for ENS-FUT, respectively; Table S3). The ITCZ anomalies we diagnose in response to future LULCC are thus very small (i.e., an order of magnitude less than the horizontal resolution of the GCMs) and are nonsignificant for the ensemble mean. In consequence, teleconnections with regard to changes in cross-equatorial heat transport or ITCZ shifts in response to future LULCC (RCP8.5 scenario) are not found to be significant contributors to decreases in monsoon rainfall.

Nonetheless, local land-atmosphere interactions have also been suggested to have strong influence on monsoon rainfall patterns [*Gupta et al.*, 2005; *Pielke et al.*, 2007; *Takata et al.*, 2009; *Niyogi et al.*, 2010; *Xue et al.*, 2010; *Halder et al.*, 2015]. Here we calculated the future biophysical changes in the land energy-balance components (Figure 3a) and in land-atmosphere variables (Figure 3b). Although not significant for all variables in all monsoon regions, a general pattern in the global monsoon system appears: future LULCC lead to a decrease in evapotranspiration (L_E), an increase in sensible heat flux (H_S), an increase in incoming radiation

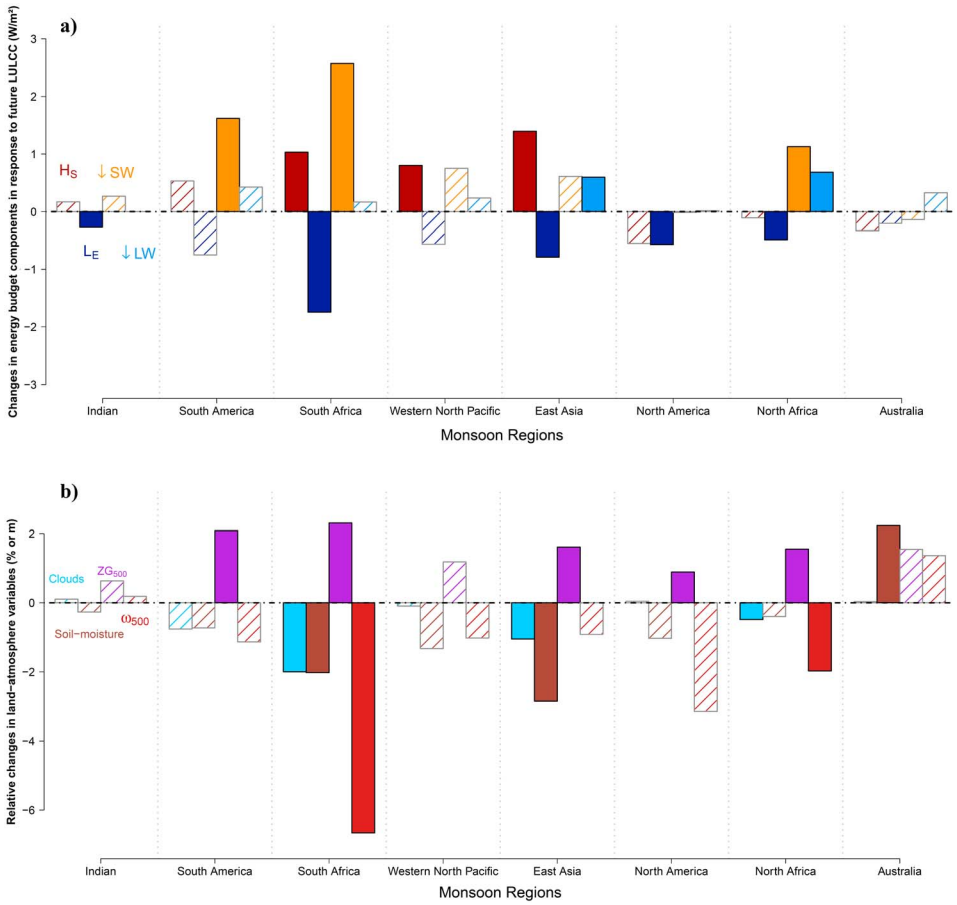

Figure 3. ENS-FUT changes in (a) land energy-balance components and (b) land-atmosphere variables in the eight monsoonal regions. For Figure 3a, changes in sensible and latent heat flux (H_s and L_E), incoming shortwave and longwave radiation at the surface (↓SW and ↓LW) are displayed and units are W/m^2. For Figure 3b, percentage changes in total cloud fraction (Clouds), soil moisture, and vertical pressure velocity at 500 hPa (ω_{500}, negative values mean subsidence) are shown and units are percent. Geopotential height at 500 hPa (ZG_{500}) is shown on the same *Y* axis but with meter units. Filled (hatched) bars depict ENS-FUT changes significant (nonsignificant) at 90th confidence level. Differences (RCP8.5-L2A85) are calculated for DJF in Southern Hemisphere regions and for JJA in Northern Hemisphere regions on 2071–2100 period.

(↓SW + ↓LW), a decrease in total cloud fraction and in soil moisture, more anticyclonic conditions (ZG_{500}), and increased tropospheric subsidence anomalies (ω_{500}), in a majority of monsoon areas (Figure 3). Future LULCC cause a change in sensible and latent heat flux partitioning by about +0.4 W/m^2 and −0.7 W/m^2 on average, respectively, significantly in South Africa and East Asia. Incoming radiation at the surface is amplified by about 1.2 W/m^2 (of which approximately three fourths is due to increased solar irradiance, ↓SW). Some changes in tropospheric circulation are found during monsoon seasons: an increase of 1.5 m in ZG_{500} and by 1.7% in subsidence anomalies (negative ω_{500} values in Figure 3). Clouds and soil moisture are found to be reduced by 0.5% and 0.8% on average. South Africa is the region that most strongly exhibits this pattern which is in line with the strongest and most significant continental precipitation decline (Figure S3). Averaged over their regional domain, few significant changes in land energy-balance components and atmospheric variables are found in Australia (only region showing an increase in continental precipitation and a south-north dipole, Figure S3) and in Indian region (aggregation of two different land and ocean responses, Figure 2 for $Indian_{JJA}$). A special focus on the Indian monsoon is performed to detail its regional specificity. The use of other larger Indian domains found in the literature (Figure S8) leads to more sensitive results with larger changes in absolute rainfall (between [−1.4%; −1.8%] versus −1% here) and a larger contribution of LULCC to Indian monsoon rainfall projections ([−11; −14%] versus −9% here) than the ones presented here. In addition, significant and substantial changes in land-atmosphere

interactions are found in the Eastern India/Bangladesh region (Figure S9) but few elsewhere within the Indian domain.

Thus, a coherent local land-atmosphere feedback, comparable to the one proposed by *Xu et al*. [2015], is found to be a significant contributor to reduction in monsoon rainfall: deforestation leads to reduce water interception, infiltration capacity, and evapotranspiration flux; decreases the water vapor amount to form clouds which in turn increases incoming radiation; and favors anticyclonic conditions and subsidence anomalies that further prevent local precipitation recycling and enhance surface drying.

4. Conclusion

LULCC-biophysical impacts on rainfall in each monsoon region are now assessed as realistically as possible given current knowledge and global coupled modeling capabilities. By using multimodel simulations, based on common global and realistic LULCC scenarios, our attribution analysis reveals that biophysical effects of LULCC have a substantial drying role in monsoon regions. We quantify that they could weaken past and future changes in monsoon rainfall by about one third on average. As only approximately two thirds of global climate models account for LULCC [*IPCC*, 2013], the current average projections of monsoon rainfall could be overestimated. The underlying physical mechanisms imply a modulation of land-atmosphere interactions (less surface moisture flux, more anticyclonic conditions) and significant changes in the local surface energy-balance components (less evapotranspiration, more incoming radiation). In consequence, a positive local soil moisture/precipitation feedback is thought to be a predominant driving mechanism rather than remote effects involving ITCZ shifts or large-scale changes in heat transport that have been put forward in recent literature. As the LULCC-biophysical effects are almost immediate compared to biogeochemical effects (e.g., progressive CO_2 release), taking into account LULCC accurately could improve the forecast skill of monsoon rainfall on interannual and multidecadal time scales [*Wang et al*., 2015]. Note that our study does not include the simulation of the irrigation potential, land management, and urbanization. These land use changes are also found to modulate the hydrological cycle [*Pielke et al*., 2011; *Mahmood et al*., 2014]. Moreover, our results are established using simulations of relatively coarse spatial resolution, and regional modeling analysis could improve the representation of the hydrological cycle in monsoon regions [e.g., *Xue et al*., 2016]. To increase confidence and robustness in monsoon projections and climate mitigation strategies, we stress here the importance of considering carefully LULCC for future projections of the hydrological cycle.

Acknowledgments
This work is performed in the framework of the EC FP7 LUC4C project (http://luc4c.eu, grant 603542). The authors thank the data producers' from LUCID (http://www.lucidproject.org.au/) and LUCID-CMIP5 projects (https://www.mpimet.mpg.de/en/science/the-land-in-the-earth-system/working-groups/climate-biogeosphere-interaction/lucid-cmip5/): Vivek Arora, Juan-Pablo Boisier, Victor Brovkin, Patricia Cadule, Veronika Gayler, Etsushi Kato, Andy Pitman, Julia Pongratz, and Eddy Robertson, for making available their model outputs and for their contribution. We also acknowledge the World Climate Research Programme's Working Group on Coupled Modeling, which is responsible for CMIP5 (http://cmip-pcmdi.llnl.gov/cmip5), and the climate modeling groups (listed in Table S3 of this paper).

References

Abiodun, B. J., J. S. Pal, E. A. Afiesimama, W. J. Gutowski, and A. Adedoyin (2008), Simulation of West African monsoon using RegCM3 Part II: Impacts of deforestation and desertification, *Theor. Appl. Climatol.*, *93*(3–4), 245–261, doi:10.1007/s00704-007-0333-1.

Adam, O., T. Bischoff, and T. Schneider (2016), Seasonal and interannual variations of the energy flux equator and ITCZ. Part I: Zonally averaged ITCZ position, *J. Clim.*, *29*(9), 3219–3230, doi:10.1175/JCLI-D-15-0512.1.

Auffhammer, M., V. Ramanathan, and J. R. Vincent (2012), Climate change, the monsoon, and rice yield in India, *Clim. Change*, *111*(2), 411–424, doi:10.1007/s10584-011-0208-4.

Avissar, R., and D. Werth (2005), Global hydroclimatological teleconnections resulting from tropical deforestation, *J. Hydrometeorol.*, *6*(2), 134–145, doi:10.1175/JHM406.1.

Badger, A. M., and P. A. Dirmeyer (2015), Remote tropical and sub-tropical responses to Amazon deforestation, *Clim. Dyn.*, *1–10*, doi:10.1007/s00382-015-2752-5.

Boisier, J. P., N. de Noblet-Ducoudré, A. J. Pitman, F. T. Cruz, C. Delire, B. J. J. M. van den Hurk, M. K. van der Molen, C. Müller, and A. Voldoire (2012), Attributing the impacts of land-cover changes in temperate regions on surface temperature and heat fluxes to specific causes: Results from the first LUCID set of simulations, *J. Geophys. Res.*, *117*, D12116, doi:10.1029/2011JD017106.

Boysen, L. R., V. Brovkin, V. K. Arora, P. Cadule, N. de Noblet-Ducoudré, E. Kato, J. Pongratz, and V. Gayler (2014), Global and regional effects of land-use change on climate in 21st century simulations with interactive carbon cycle, *Earth Syst. Dyn.*, *5*(2), 309–319, doi:10.5194/esd-5-309-2014.

Brovkin, V., et al. (2013), Effect of anthropogenic land-use and land-cover changes on climate and land carbon storage in CMIP5 projections for the twenty-first century, *J. Clim.*, *26*(18), 6859–6881, doi:10.1175/JCLI-D-12-00623.1.

Chase, T. N., R. A. P. Sr, T. G. F. Kittel, R. R. Nemani, and S. W. Running (2000), Simulated impacts of historical land cover changes on global climate in northern winter, *Clim. Dyn.*, *16*(2–3), 93–105, doi:10.1007/s003820050007.

Devaraju, N., G. Bala, and A. Modak (2015), Effects of large-scale deforestation on precipitation in the monsoon regions: Remote versus local effects, *Proc. Natl. Acad. Sci. U.S.A.*, *112*(11), 3257–3262, doi:10.1073/pnas.1423439112.

Donohoe, A., J. Marshall, D. Ferreira, K. Armour, and D. McGee (2014), The interannual variability of tropical precipitation and interhemispheric energy transport, *J. Clim.*, *27*(9), 3377–3392, doi:10.1175/JCLI-D-13-00499.1.

Feddema, J. J., K. W. Oleson, G. B. Bonan, L. O. Mearns, L. E. Buja, G. A. Meehl, and W. M. Washington (2005), The importance of land-cover change in simulating future climates, *Science*, *310*(5754), 1674–1678, doi:10.1126/science.1118160.

Findell, K. L., T. R. Knutson, and P. C. D. Milly (2006), Weak simulated extratropical responses to complete tropical deforestation, *J. Clim.*, *19*(12), 2835–2850, doi:10.1175/JCLI3737.1.

Findell, K. L., A. J. Pitman, M. H. England, and P. J. Pegion (2009), Regional and global impacts of land cover change and sea surface temperature anomalies, *J. Clim.*, *22*(12), 3248–3269, doi:10.1175/2008JCLI2580.1.
Gadgil, S., and S. Gadgil (2006), The Indian monsoon, GDP and agriculture, *Econ. Polit. Wkly.*, *41*(47), 4887–4895.
Goldewijk, K. K. (2001), Estimating global land use change over the past 300 years: The HYDE database, *Global Biogeochem. Cycles*, *15*, 417–433, doi:10.1029/1999GB001232.
Gupta, A., P. K. Thapliyal, P. K. Pal, and P. C. Joshi (2005), Impact of deforestation on Indian monsoon—A GCM sensitivity study, *J. Indian Geophys. Union*, *9*(2), 97–104.
Haensler, A., F. Saeed, and D. Jacob (2013), Assessing the robustness of projected precipitation changes over central Africa on the basis of a multitude of global and regional climate projections, *Clim. Change*, *121*(2), 349–363, doi:10.1007/s10584-013-0863-8.
Halder, S., S. K. Saha, P. A. Dirmeyer, T. N. Chase, and B. N. Goswami (2015), Investigating the impact of land-use land-cover change on Indian summer monsoon daily rainfall and temperature during 1951–2005 using a regional climate model, *Hydrol. Earth Syst. Sci. Discuss.*, *12*(7), 6575–6633, doi:10.5194/hessd-12-6575-2015.
Held, I. M., and B. J. Soden (2006), Robust responses of the hydrological cycle to global warming, *J. Clim.*, *19*(21), 5686–5699, doi:10.1175/JCLI3990.1.
Hollander, M., and D. A. Wolfe (1999), *Nonparametric Statistical Methods*, 2nd ed., Wiley-Interscience, New York.
Hurtt, G. C., et al. (2011), Harmonization of land-use scenarios for the period 1500–2100: 600 years of global gridded annual land-use transitions, wood harvest, and resulting secondary lands, *Clim. Change*, *109*(1–2), 117–161, doi:10.1007/s10584-011-0153-2.
Intergovernmental Panel on Climate Change (IPCC) (2013), *Climate Change 2013: The Physical Science Basis. Contribution of Working Group I to the Fifth Assessment Report of the Intergovernmental Panel on Climate Change*, edited by T. F. Stocker et al., 1535 pp., Cambridge Univ. Press, Cambridge, U. K., and New York, doi:10.1017/CBO9781107415324.
Jacob, D., et al. (2014), EURO-CORDEX: New high-resolution climate change projections for European impact research, *Reg. Environ. Change*, *14*(2), 563–578, doi:10.1007/s10113-013-0499-2.
Kishtawal, C. M., D. Niyogi, M. Tewari, R. A. Pielke, and J. M. Shepherd (2010), Urbanization signature in the observed heavy rainfall climatology over India, *Int. J. Climatol.*, *30*(13), 1908–1916, doi:10.1002/joc.2044.
Kitoh, A., H. Endo, K. Krishna Kumar, I. F. A. Cavalcanti, P. Goswami, and T. Zhou (2013), Monsoons in a changing world: A regional perspective in a global context, *J. Geophys. Res. Atmos.*, *118*, 3053–3065, doi:10.1002/jgrd.50258.
Lawrence, D., and K. Vandecar (2015), Effects of tropical deforestation on climate and agriculture, *Nat. Clim. Change*, *5*(1), 27–36, doi:10.1038/nclimate2430.
Lee, E., T. N. Chase, B. Rajagopalan, R. G. Barry, T. W. Biggs, and P. J. Lawrence (2009), Effects of irrigation and vegetation activity on early Indian summer monsoon variability, *Int. J. Climatol.*, *29*(4), 573–581, doi:10.1002/joc.1721.
Lee, J.-Y., and B. Wang (2014), Future change of global monsoon in the CMIP5, *Clim. Dyn.*, *42*(1–2), 101–119, doi:10.1007/s00382-012-1564-0.
Mahmood, R., et al. (2014), Land cover changes and their biogeophysical effects on climate, *Int. J. Climatol.*, *34*(4), 929–953, doi:10.1002/joc.3736.
McGee, D., A. Donohoe, J. Marshall, and D. Ferreira (2014), Changes in ITCZ location and cross-equatorial heat transport at the Last Glacial Maximum, Heinrich Stadial 1, and the mid-Holocene, *Earth Planet. Sci. Lett.*, *390*, 69–79, doi:10.1016/j.epsl.2013.12.043.
Medvigy, D., R. L. Walko, and R. Avissar (2010), Effects of deforestation on spatiotemporal distributions of precipitation in South America, *J. Clim.*, *24*(8), 2147–2163, doi:10.1175/2010JCLI3882.1.
Niyogi, D., C. Kishtawal, S. Tripathi, and R. S. Govindaraju (2010), Observational evidence that agricultural intensification and land use change may be reducing the Indian summer monsoon rainfall, *Water Resour. Res.*, *46*, W03533, doi:10.1029/2008WR007082.
de Noblet-Ducoudré, N., et al. (2012), Determining robust impacts of land-use-induced land cover changes on surface climate over North America and Eurasia: Results from the first set of LUCID experiments, *J. Clim.*, *25*(9), 3261–3281, doi:10.1175/JCLI-D-11-00338.1.
Pfeifer, S., K. Bülow, A. Gobiet, A. Hänsler, M. Mudelsee, J. Otto, D. Rechid, C. Teichmann, and D. Jacob (2015), Robustness of ensemble climate projections analyzed with climate signal maps: Seasonal and extreme precipitation for Germany, *Atmosphere*, *6*(5), 677–698, doi:10.3390/atmos6050677.
Pielke, R. A., J. Adegoke, A. BeltráN-Przekurat, C. A. Hiemstra, J. Lin, U. S. Nair, D. Niyogi, and T. E. Nobis (2007), An overview of regional land-use and land-cover impacts on rainfall, *Tellus B*, *59*(3), 587–601, doi:10.1111/j.1600-0889.2007.00251.x.
Pielke, R. A., et al. (2011), Land use/land cover changes and climate: Modeling analysis and observational evidence, *Wiley Interdiscip. Rev. Clim. Change*, *2*(6), 828–850, doi:10.1002/wcc.144.
Pitman, A. J., et al. (2009), Uncertainties in climate responses to past land cover change: First results from the LUCID intercomparison study, *Geophys. Res. Lett.*, *36*, L14814, doi:10.1029/2009GL039076.
Ramankutty, N., and J. A. Foley (1999), Estimating historical changes in global land cover: Croplands from 1700 to 1992, *Global Biogeochem. Cycles*, *13*, 997–1027, doi:10.1029/1999GB900046.
Smith, M. C., J. S. Singarayer, P. J. Valdes, J. O. Kaplan, and N. P. Branch (2016), The biogeophysical climatic impacts of anthropogenic land use change during the Holocene, *Clim. Past*, *12*(4), 923–941, doi:10.5194/cp-12-923-2016.
Snyder, P. K. (2010), The influence of tropical deforestation on the Northern Hemisphere climate by atmospheric teleconnections, *Earth Interact.*, *14*(4), 1–34, doi:10.1175/2010EI280.1.
Swann, A. L. S., I. Y. Fung, and J. C. H. Chiang (2012), Mid-latitude afforestation shifts general circulation and tropical precipitation, *Proc. Natl. Acad. Sci. U.S.A.*, *109*(3), 712–716, doi:10.1073/pnas.1116706108.
Takata, K., K. Saito, and T. Yasunari (2009), Changes in the Asian monsoon climate during 1700–1850 induced by preindustrial cultivation, *Proc. Natl. Acad. Sci. U.S.A.*, *106*(24), 9586–9589, doi:10.1073/pnas.0807346106.
Thober, S., and L. Samaniego (2014), Robust ensemble selection by multivariate evaluation of extreme precipitation and temperature characteristics, *J. Geophys. Res. Atmos.*, *119*, 594–613, doi:10.1002/2013JD020505.
Tiwari, P. C., and B. Joshi (2013), Changing monsoon pattern and its impact on water resources in Himalaya, in *Climate Adaptation Futures*, edited by J. Palutikof et al., pp. 301–307, John Wiley, Chichester, U. K.
Trenberth, K. (2011), Changes in precipitation with climate change, *Clim. Res.*, *47*(1), 123–138, doi:10.3354/cr00953.
Trenberth, K. E., D. P. Stepaniak, and J. M. Caron (2000), The global monsoon as seen through the divergent atmospheric circulation, *J. Clim.*, *13*(22), 3969–3993, doi:10.1175/1520-0442(2000)013<3969:TGMAST>2.0.CO;2.
Wang, B., and Q. Ding (2006), Changes in global monsoon precipitation over the past 56 years, *Geophys. Res. Lett.*, *33*, L06711, doi:10.1029/2005GL025347.
Wang, B., and Q. Ding (2008), Global monsoon: Dominant mode of annual variation in the tropics, *Dyn. Atmos. Oceans*, *44*(3–4), 165–183, doi:10.1016/j.dynatmoce.2007.05.002.

Wang, B., and LinHo (2002), Rainy season of the Asian–Pacific summer monsoon*, *J. Clim.*, *15*(4), 386–398, doi:10.1175/1520-0442(2002)015<0386:RSOTAP>2.0.CO;2.

Wang, B., B. Xiang, J. Li, P. J. Webster, M. N. Rajeevan, J. Liu, and K.-J. Ha (2015), Rethinking Indian monsoon rainfall prediction in the context of recent global warming, *Nat. Commun.*, *6*, 7154, doi:10.1038/ncomms8154.

Ward, D. S., N. M. Mahowald, and S. Kloster (2014), Potential climate forcing of land use and land cover change, *Atmos. Chem. Phys.*, *14*(23), 12,701–12,724, doi:10.5194/acp-14-12701-2014.

Webb, T. J., F. I. Woodward, L. Hannah, and K. J. Gaston (2005), Forest cover–rainfall relationships in a biodiversity hotspot: The Atlantic forest of Brazil, *Ecol. Appl.*, *15*(6), 1968–1983, doi:10.1890/04-1675.

Werth, D., and R. Avissar (2002), The local and global effects of Amazon deforestation, *J. Geophys. Res.*, *107*(D20), 8087, doi:10.1029/2001JD000717.

Xu, Z., R. Mahmood, Z.-L. Yang, C. Fu, and H. Su (2015), Investigating diurnal and seasonal climatic response to land use and land cover change over monsoon Asia with the Community Earth System Model, *J. Geophys. Res. Atmos.*, *120*, 1137–1152, doi:10.1002/2014JD022479.

Xue, Y., and P. Dirmeyer (2015), Land-atmosphere interactions in monsoon regimes and future prospects for enhancing prediction, *CLIVAR Exch. Newsl.*, *19*, 28.

Xue, Y., F. De Sales, R. Vasic, C. R. Mechoso, A. Arakawa, and S. Prince (2010), Global and seasonal assessment of interactions between climate and vegetation biophysical processes: A GCM study with different land–vegetation representations, *J. Clim.*, *23*(6), 1411–1433, doi:10.1175/2009JCLI3054.1.

Xue, Y., et al. (2016), West African monsoon decadal variability and surface-related forcings: Second West African Monsoon Modeling and Evaluation Project Experiment (WAMME II), *Clim. Dyn.*, *47*, 3517–3545, doi:10.1007/s00382-016-3224-2.

Yim, S.-Y., B. Wang, J. Liu, and Z. Wu (2014), A comparison of regional monsoon variability using monsoon indices, *Clim. Dyn.*, *43*(5–6), 1423–1437, doi:10.1007/s00382-013-1956-9.

Zhang, H., A. Henderson-Sellers, and K. McGuffie (1996), Impacts of tropical deforestation. Part II: The role of large-scale dynamics, *J. Clim.*, *9*(10), 2498–2521, doi:10.1175/1520-0442(1996)009<2498:IOTDPI>2.0.CO;2.

Zheng, X., and E. A. B. Eltahir (1997), The response to deforestation and desertification in a model of West African monsoons, *Geophys. Res. Lett.*, *24*, 155–158, doi:10.1029/96GL03925.